Building a Kinetic Framework for Group II Intron Ribozyme Activity: Quantitation of Interdomain Binding and Reaction Rate†

Anna Marie Pyle* and Justin B. Green

Department of Biochemistry and Molecular Biophysics, Columbia University College of Physicians and Surgeons, New York, New York 10032

Received September 15, 1993; Revised Manuscript Received November 22, 1993®

ABSTRACT: Ribozyme kinetics and binding studies of a two-piece group II intron were used to mechanistically characterize a reaction analogous to the first step of RNA splicing. Domain 5 RNA (D5) catalyzes specific hydrolysis of an RNA substrate (exD123) composed of sequences surrounding the 5′ exon/intron boundary. Both single- and multiple-turnover kinetic analyses produced similar values of k_{cat} (0.04 and 0.1 min^{-1}, respectively) and K_m (270 and 190 nM, respectively) for 5′ splice site hydrolysis catalyzed by D5. Base pairing is not believed to stabilize the binding of D5 to exD123, so the low K_m values suggest that unusual tertiary interactions provide considerable energetic stabilization to this complex. The strength of D5–exD123 binding was confirmed using a new direct binding assay based on gel filtration chromatography. In this initial application of the assay, which systematically underestimates binding by approximately 3-fold, K_d values were obtained in relative agreement with K_m. This agreement, together with agreement between kinetically determined variables, suggests that the reaction is described by a straightforward Michaelis–Menten mechanism and that k_{cat} is the rate of the chemical step. This is supported by the log/linear pH/rate profile for k_{cat} which has a slope = 1 up to pH 6.2, consistent with a form of general base cataysis within this linear range. The shape of the plot suggests that the active site responsible for 5′ splice site hydrolysis has a pK_a of ≥7.0.

The ai5γ group II intron is an autocatalytic RNA that is capable of excising itself from precursor RNA and ligating the flanking pieces without assistance from protein enzymes (Peebles et al., 1986). Group II introns are involved in processing certain organellar genes in yeast and higher plants (Michel et al., 1989; Wissinger et al., 1992). Particular interest has recently centered on group II intron self-splicing as a model for spliceosomal RNA splicing in eukaryotes because both forms of RNA processing result in exon ligation with concomitant release of a lariat-shaped intron product (Sharp, 1985, 1988; Cech, 1986). Although group II introns can catalyze this reaction autonomously, pre-mRNA splicing requires a host of protein cofactors and a set of five small nuclear RNAs (Guthrie, 1991; Moore et al., 1993). The contiguous RNA composing the group II intron can be arranged into a set of six domains, of which domains 1, 5, and 6 appear to be essential for catalytic activity (Figure 1a) (Kwakman et al., 1989; Bachl & Schmelzer, 1990; Jacquier & Jacquesson-Breuleux, 1991; Koch et al., 1992). It has been proposed that these domains might function in a manner analogous to small nuclear RNAs within the eukaryotic splicing apparatus (Weiner, 1987; Madhani & Guthrie, 1992). Although the catalytically essential domains must fold and assemble together in formation of the group II intron active site, there is no readily apparent phylogenetic covariation between the domains, suggesting that the interactions responsible for organizing them into an active structure do not involve base pairing (Michel et al., 1989). Few nucleotides within the expansive group II intron are phylogenetically conserved and most of these residues fall within a small hairpin structure known as domain 5 (D5)[1] (Figure 1a,b) (Michel et al., 1989). This base-paired region is believed to be an essential component of the active site because it can promote hydrolysis of the 5′ splice site when added in trans to segments of the exon–intron boundary (Figure 1c) (Jarrell et al., 1988a). Although group II intron splicing is usually initiated by nucleophilic attack of the branch-point adenosine, splicing can proceed properly when the first step involves a hydrolysis reaction (using water as the nucleophile) if the bulged A in domain 6 is inactivated through base pairing (van der Veen et al., 1987). In the full-length intron, hydrolysis of the 5′ splice site (rather than adenosine attack) is readily activated by high concentrations of KCl. Under these conditions, the hydrolyzed 5′-exon participates in the second step with release of ligated exons (Jarrell et al., 1988b). The 5′ splice site hydrolysis reaction is relevant to splicing and can take place using only pieces of the group II intron. This mechanistic simplication of the first step of splicing makes it possible to study the reaction enzymologically. A recent proposal suggests that group II intron splicing may be most closely related to the spliceosomal mechanism during the first step of splicing (Moore et al., 1993). If this hypothesis is true, then characterization of the mechanistically straightforward first step could help build a foundation for models of nuclear pre-mRNA splicing. Our understanding of this reaction requires characterization of the interactions between domain 5 and domains adjacent to the 5′ splice site. The fact that the interdomain associations cannot be understood using contemporary models for RNA folding also makes the group II

† This work was supported by a seed grant from the American Cancer Society and the Irma T. Hirschl Fund for Medical Research.

* Author to whom correspondence should be addressed.

® Abstract published in *Advance ACS Abstracts,* February 1, 1994.

[1] Abbreviations: D5, domain 5 of the group II intron; exD123, the 5′-exon and domains 1–3 of the group II intron; K_m(ST), the apparent dissociation constant of the D5–exD123 complex from single-turnover kinetics; K_m(MT), the Michaelis constant from multiple-turnover kinetics; K_d, the dissociation constant measured using direct methods; k_{chem}, the rate constant for the chemical step, presumed to equal k_{cat} values from both single- and multiple-turnover kinetics; nts, nucleotides.

0006-2960/94/0433-2716$04.50/0

intron an interesting example of RNA tertiary structural organization.

A serious impediment to our understanding of group II intron organization is a lack of kinetic information about its function and the lack of methodologies for studying its tertiary interactions. Without a kinetic and structural framework for the group II intron, it will be difficult to interpret the effects of mutations, deletions, or backbone modifications necessary for dissecting the function of the intron. The lack of data on interdomain association constants has complicated the initiation of spectroscopic and biochemical mapping studies that would elucidate tertiary architecture. For this reason, we have undertaken a study that provides a coherent kinetic framework for the first step of splicing stimulated by domain 5 of the group II intron. Using two independent kinetic approaches to 5′ splice site hydrolysis, a new method for quantitating the energetics of interdomain interactions, and a series of pH/rate profiles, we have isolated individual rate and binding constants that may be important to group II intron activity. Although mechanistic conclusions about the 5′ splice site hydrolysis reaction may not apply to the normal self-splicing reaction, it is likely that many of the RNA structures and catalytic mechanisms that promote nucleophilic attack of water at the 5′ splice site may also promote the adenosine attack characteristic of autocatalytic and spliceosomal processing. Therefore, we believe this simplified system provides a valuable approach for studying the group II intron active site.

The study was performed using a two-piece group II intron. One of the RNAs contains 5′-exon sequences and domains 1–3 of the intron (exD123, Figure 1a,c) while the other is composed of the domain 5 RNA (D5, Figure 1a,b). By treating the longer RNA as a reaction "substrate" and the shorter RNA as an "enzyme", it has been possible to resolve the chemical rate of 5′ splice site hydrolysis from individual subdomain binding events. This kinetically tractable reaction provides a convenient window on group II intron reactivity and structure.

MATERIALS AND METHODS

Materials. Deletion constructs of the ai5γ intron from the *oxi* 3 gene of yeast mitochondrial DNA (plasmids pJDI3′-673 and pJDI5′-75) were kindly provided by the laboratory of Philip S. Perlman (Jarrell et al., 1988a). Plasmids were amplified and checked by sequencing before use in transcription. T7 RNA polymerase, a gift from Dr. Nancy Greenbaum, was prepared using literature procedures (Davanloo et al., 1984). Nucleotide triphosphates were purchased from Pharmacia. Only ultrapure $MgCl_2$ (Aldrich 99.999%) was utilized in these experiments to prevent RNA precipitation by impurities.

DNA Constructs and RNA Transcription. The exD123 RNA (1003 nt total; containing 293 nucleotides of 5′-exon joined to domains 1–3) was transcribed from plasmid pJDI3′-673 linearized with *Hind*III. D5 RNA (58 nt total; containing domain 5 flanked by 22 vector-derived nucleotides) was transcribed from pJDI5′-75 linearized with *Hpa*II. RNA internally labeled with ^{32}P was transcribed with α-^{32}P-UTP in a volume of 20 μL (Been & Cech, 1987). Unlabeled cold RNAs were transcribed in 2 mL, purified by PAGE, and UV-shadowed (Zaug et al., 1988). After purification, samples were stored frozen in MOPS [3-(*N*-morpholino)propanesulfonic acid] pH 6.5 (10 mM), EDTA (1 mM). For nonradioactive RNAs, concentrations were determined spectrophotometrically using extinction coefficients at 260 nm ($\epsilon_{260\ nm}$) of 6.4×10^5 M^{-1} cm^{-1} for D5 and 1×10^7 M^{-1} cm^{-1} for exD123. Extinction coefficients were determined by adding ϵ_{260} values of component nucleotides at pH 7.0. Absorbances were measured in the absence of salt to minimize the optical effects of base-stacking hypochromicity. The secondary structure stabilized by salt causes a downward deviation of up to 30% from the average $\epsilon_{260\ nm}$ per residue of approximately 1×10^4 M^{-1} cm^{-1} (Cantor & Schimmel, 1980, p 384 and 399). The concentrations of radioactive RNAs were determined from their specific activities.

Reaction Conditions for Cleavage of exD123 RNA. Reactions were performed in 0.65-mL RNAse-free siliconized tubes (National Scientific) in a total volume of 20 μL. Standard reaction and binding buffer contained 40 mM tris or MOPS (pH 7.5), 100 mM $MgCl_2$, and 500 mM KCl. All reactions were carried out using the following protocol: RNA stock solutions (in 40 mM MOPS) were diluted separately and preincubated at 95 °C for 1 min in order to eliminate alternative RNA conformations which may have formed during storage at −20 °C (Groebe & Uhlenbeck, 1988; Walstrum & Uhlenbeck, 1990; Fedor & Uhlenbeck, 1992). After RNAs had cooled below 45 °C, reactions were initiated by combining D5 and exD123 RNA with simultaneous addition of 100 mM $MgCl_2$ and 500 mM KCl (final concentrations) and incubating at 45 °C. Reaction rate was not enhanced by adding salts to preincubated D5 or exD123 individually, thus allowing them to "prefold" at 45 °C, before the RNAs were combined. For single-turnover kinetics (D5 excess), ^{32}P-exD123 was used at a concentration of 1 nM. The concentration of D5 was varied from 0.05 to 6 μM. Reactions were incubated at 45 °C from 0 to 180 min. At each timepoint, 2-μL aliquots were removed from each reaction, quenched with a denaturing dye solution, and chilled before loading onto a 4% denaturing polyacrylamide gel. After electrophoresis and drying of the gel, the reaction products were visualized by autoradiography and quantitated on a Betascope radioanalytic detector (Betagen). For multiple-turnover kinetics (exD123 excess), the [D5] was 5 nM and [exD123] was varied from 20 to 250 nM. To visualize the reaction course, the exD123 mix was spiked with 1 nM ^{32}P-exD123. Reactions were quantitated as described above.

Kinetics. Single-turnover kinetics: Reactions were performed using trace concentrations of ^{32}P-body-labeled exD123 (as substrate) and an excess of D5 RNA (as enzyme). Reaction extent was monitored by calculating the fraction of product at each timepoint. In order to minimize effects of differential RNA degradation with varying reaction times, fraction of product was computed for each lane by dividing the product counts (normalized for molecular size and corrected for background) by the counts of substrate + product. Reaction rates (k_{obs}) were obtained by plotting the natural log of substrate remaining (or 1 − fraction product) vs time. As expected for a reaction obeying pseudo-first-order kinetics, there was no dependence of k_{obs} on [exD123] in the subsaturating range tested (0.3 to 3 nM). Pseudo-first-order plots were linear for greater than three half-lives of reaction at saturating concentrations of D5 and trace concentrations of exD123. When an arbitrary endpoint of 95% reaction was chosen, all plots were linear for more than five half-lives of reaction. Amounts of product and substrate were not corrected to account for an inactive subpopulation because reaction extent was greater than 95% (> four reaction half-lives). In addition, assignment of a precise endpoint for correcting pseudo-first-order plots is complicated by the large size of exD123, which undergoes a competing random hydrolysis reaction at long times. This degradation is normal for large RNAs at 100 mM Mg^{2+} and 45 °C reaction temperatures.

To minimize spurious effects of RNA degradation, especially on rate constants for slower reactions at pH 7.5 (such as those at subsaturating concentrations of D5), rate constants used in single-turnover K_m(ST) determination were obtained using timepoints of no longer than 1 h. Error in the k_{obs} values was obtained by comparing three time courses at the same [D5]. Values in k_{obs} were found to vary by ±18% (with 95% confidence) for experiments performed several days apart. Multiple-turnover kinetics (Fedor & Uhlenbeck, 1990; Herschag & Cech, 1990a): Rates of reaction at six different concentrations were studied with two repetitions. Because random degradation increased radically with each timepoint (due to long incubation times and low signal), it was necessary to subtract background counts unique to each lane and reaction condition. This was achieved by using the normalized counts from the space above each product band (quantitated as equal areas) as a measure of background. Initial rates were obtained by first plotting the [product generated] vs time for each [D1]. The slopes of these linear plots (k_{obs} values) were used to generate an Eadie-Hofstee plot with slope = $-K_m$ and intercept = k_{cat}([D5]). Although measured variation in kinetic constants was typically low for experiments performed just days apart, kinetic parameters were found to vary up to 2-fold for experiments performed months apart using entirely different RNA stocks, as is typical for studies of ribozyme kinetics (Herschlag & Cech, 1990a; Fedor & Uhlenbeck, 1992). We therefore expect that 2-fold variations in k_{cat} and K_m are insignificant for experiments performed months apart using different experimental approaches that are inherently sensitive to different sources of experimental error (such as single- and multiple-turnover kinetics).

Gel-Filtration Binding Assay. Sephacryl S-100 (Sigma) was prepared in reaction buffer (40 mM tris, pH 7.5, 100 mM $MgCl_2$, 500 mM KCl) and autoclaved. The column (a 10-mL Falcon serological pipet) was plugged with siliconized glass wool and packed with 8 mL of sephacryl support. After each RNA component was preincubated at 95 °C for 1 min (in 10 mM MOPS pH 7.5), RNAs were combined together with reaction buffer in a total volume of 20 μL. This sample was incubated at 45 °C for 5 min, loaded directly onto the bed of the column, and eluted with slight air pressure at a flow-rate of approximately 1 mL/min at 25 °C. D5–exD123 complex eluted in approximately 2 min, immediately after the void volume. Fraction volumes of 100 μL were taken during elution and collected directly into scintillation vials. Counts/fraction were determined by Cerenkov scintillation counting. Bound vs free ^{32}P-D5 was plotted, and a curve was drawn through the points, representing the nonlinear least-squares fit to an equation describing 1:1 molecular association. This equation, which describes the simplest isotherm for bimolecular association, is identical to that used in previous studies of substrate binding to the *Tetrahymena* ribozyme (Pyle et al., 1990; Pyle & Cech, 1991) and is based on the following definitions:

$$K_d = [D5][exD123]/[D5{\cdot}exD123]$$

$$\Theta, \text{ or fraction D5 bound} = [D5{\cdot}exD123]/[D5]_{total}$$

$$[exD123] = [exD123]_{total} - [D5{\cdot}exD123] = [exD123]_{total} - (\Theta)([D5]_{total})$$

The terms are arranged to solve for only one experimentally determined variable (fraction D5 bound, or Θ) in terms of K_d and the experimentally known quantities $[D5]_{total}$ and $[exD123]_{total}$. Where t = total, the equation which results from such a treatment is

$$\Theta = ([D5]_t + [exD123]_t + K_d - \text{sqrt}\,[([D5]_t + [exD123]_t + K_d)^2 - 4[D5]_t\,[exD123]_t)]/2[D5]_t$$

This equation was entered into a curve-fit program and standard error was calculated from the fit of the observed curve to the theoretical one described by this isotherm. Values for the standard error derived from the covariance matrix (Press et al., 1992) (reported by curve-fit programs such as Kaleidagraph simply as "error" for the floating variable K_d) are shown in Table 1. The applicability of a covariance matrix for determination of standard error was confirmed using a jackknife approximation of the standard error (Mosteller & Tukey, 1977), which produced values that were in close agreement. Data were corrected for apparent 5% inactive populations of D5 and GGCCCGCU. Quantity of inactive ligand was determined from best fits to the binding isotherm which has, by definition, an asymptote of 1 at infinite macromolecular concentration. Small inactive populations of 5% are commonly due either to errors in transcription or folding and can vary from one preparation to the next.

pH/Rate Determinations. Rate constants were obtained under single turnover conditions with saturating [D5] (3 μM) and trace [exD123] (1 nM) in experiments from pH 5.0 to 9.0. Multiple buffers were required to survey the range from pH 5.0 to 9.0, so wherever possible, reactions were studied in two buffers of overlapping pH range. No dependence on buffer type was observed.

RESULTS

Characterization of Reaction Products. Initial reports of the reaction schematized in Figure 1c were complicated by the presence of a dominant fragment (approximately 560 nts in length) which did not correspond to either of the expected reaction products (Jarrell et al., 1988a). A time course for the reaction schematized in Figure 1c is shown in Figure 2. As reported previously, exD123 (band A) is cleaved, forming the 710 nt intron fragment (band B) and a 293 nt 5′-exon fragment (band D). In this case, however, a 560 nucleotide fragment (C) is found to evolve together with an additional fragment of approximately 150 nucleotides in length (band E). The sum of 560 and 150 nucleotides is 710 nucleotides, suggesting that these products are secondary reactions of the intron fragment. This result is consistent with a recent study which mapped the second cleavage site to a position between domains 2 and 3 of the exD123 molecule (Franzen et al., 1993). The time course shown in Figure 2 indicates that the secondary products (bands C and E) form only after the primary intron product (B) has significantly accumulated. This suggests that their formation occurs after 5′ splice site hydrolysis and does not complicate the rate of this first reaction. Consistent with this hypothesis, combination of counts from bands C and E with band B produces a kinetic profile that is the exact inverse of precursor disappearance and which is indistinguishable from that obtained by monitoring appearance of band D, the 5′-exon product (Figure 3a). That each of these curves intersect at 50% reaction indicates that a kinetic description of the 5′ splice site hydrolysis reaction need not be complicated by the secondary reaction and that all reaction products are accounted for.

Rate Constants from Single-Turnover Kinetics. This approach treats D5 as the "enzyme" and exD123 as the reaction "substrate", since the latter molecule contains the cleavage site and D5 is unchanged in the reaction. Although catalytically important functions are provided by portions of the exD123 molecule, this does not compromise the kinetic validity of the approach because substrate functional groups that are

Table 1: Kinetic Parameters Describing the Cleavage of exD123 Catalyzed by D5

parameter	single-turnover kinetics	multiple-turnover kinetics	direct binding assay
K_m (nM)	270 ± 25[a,d]	190 ± 72[b,d]	
k_{chem} (min^{-1})	0.041 ± 0.001[a,d]	0.11 ± 0.028[b,d]	
k_{cat}/K_m (M^{-1} min^{-1})	(1.5 ± 0.15) × 10^5 [c]	(5.5 ± 2.5) × 10^5 [c]	
K_d (nM)			<800 ± 50[a,e]
pK_a	≥7		

[a] This standard error derived from the covariance matrix is in agreement with a jackknife estimate of the standard error (Mosteller & Tukey, 1977). Data is fit to the binding isotherm described in the caption to Figure 3b and the Materials and Methods section. [b] Variance calculated from least-squares fit to the line of an Eadie–Hofstee plot. [c] Error calculated by propagation of K_m and k_{cat} error estimates. [d] Although the errors reported here are consistent within single data sets (obtained over several days) and reflect the goodness of fit to specific mechanistic models, up to 2-fold variation in kinetic parameters was observed between experiments conducted months apart using entirely different RNA stocks. [e] The methodology used for determination of this value appears to overestimate K_d by a factor of ~3. Application of the method to a complex with a known dissociation constant yielded a 3-fold underestimation of binding strength (Figure 4d).

spatially separated from reaction sites are commonly observed to enhance catalysis by bound ribozymes (Pyle et al., 1992; Pyle, 1993). In these experiments, [^{32}P-exD123] = 1 nM and unlabeled [D5] varied from subsaturation to saturation (0.05 to 6 μM). Seven early timepoints (0–20 min) were used to calculate the apparent rate (k_{obs}) at each [D5] from the slope of a semilog plot (Figure 3b, inset). Values for k_{obs} were then plotted as a function of [D5] (Figure 3b). Data sets for the appearance of 5′-exon product (band D, Figure 2), appearance of intron product (bands B, C, and E), and disappearance of precursor (band A) were all analyzed independently and found to be in good agreement. The reaction was observed to obey Michaelis-Menten or saturation kinetics (Figure 3b). As such, a plot of reaction rate through a range of D5 concentrations fits a curve describing simple bimolecular association. The equation for the theoretical curve is described in the legend to Figure 3b. The curve generated by this single-turnover analysis can be used to extract kinetic constants analogous to K_m and k_{cat} (Jencks, 1987; Herschlag & Cech, 1990b; McConnell et al., 1993; Zaug et al., 1993). Consistent with similar experiments on other ribozymes, the concentration of D5 at half-maximum rate [K_m(ST)] represents the apparent dissociation constant for the D5-exD123 complex (Figure 3b). The plateau of the curve represents the maximum rate of reaction at D5 saturation [k_{cat}(ST)]. At D5 saturation under the reaction conditions described in Methods, all exD123 molecules are expected to be bound, rendering k_{cat}(ST) insensitive to the rate of complex association. The reaction is not allowed to turn over and, because products are denatured and separated by electrophoresis, product need not be released to be quantitated. Thus, k_{cat}(ST) does not reflect rate-limiting product release. In this way, the experiment is typically designed to measure the rate of [enzyme·substrate] → [enzyme·product]; and k_{cat}(ST) is analogous to k_{chem} if rate-limiting conformational changes do not occur in the enzyme–substrate complex. This single-turnover analysis was applied to the data in Figure 3b and a nonlinear least squares fit to the theoretical curve resulted in a K_m(ST) of 270 ± 25 nM and a k_{cat}(ST) of 0.041 ± 0.001 min^{-1} (Table 1). These values are in agreement with k_{cat}/K_m(ST) determined by plotting k_{obs} vs [D5] at low D5 concentrations and solving for the slope of the line.

Direct Measurement of D5–exD123 Binding. The K_m(ST) defines only apparent binding as reflected through catalytic activity. A direct measure of binding (K_d) would elucidate the mechanistic significance of the kinetic parameters shown in Table 1 and would facilitate the identification of tertiary interactions contributing to binding. Gel mobility shift assays of complex stability (Pyle et al., 1990) were hampered by the high salt concentrations necessary for maintaining group II intron stability. Although we detected a complex at low salt (a prerequisite for electrophoretic approaches), we were interested in developing an assay to provide information about K_d at the same salt concentrations used in determining K_m(ST). We were also interested in finding a way to quantitate the strength of RNA–RNA association at any salt concentration, in the presence of impurities, and under a variety of temperatures. To this end, gel-filtration chromatography was explored as a means for carefully separating a ^{32}P-D5–exD123 complex from free ^{32}P-D5. After first exploring the best conditions for resolving elution of ^{32}P-D5 from ^{32}P-exD123 (Figure 4a), ^{32}P-D5 was incubated with high concentrations of cold exD123 and the resultant 20-μL binding reactions were loaded on a Sephacryl S-100 column. Because of its molecular size, the ^{32}P-D5–exD123 complex eluted immediately after the void volume (just like ^{32}P-exD123) while the free ^{32}P-D5 peak eluted at its slower, normal position (Figure 4b). A series of these elutions performed as a function of [exD123] resulted in a binding curve (Figure 4c). Fitting this curve to the simplest isotherm describing bimoleular association (see Materials and Methods) resulted in a K_d of 800 ± 50 nM. This value is approximately 3-fold larger than K_m(ST) values describing D5 binding. Because this method had not been used previously as a means for quantifying RNA–RNA association energies, a control experiment was conducted using two RNAs with a well-characterized K_d of the same magnitude as the K_m(ST) for the D5–exD123 complex. The mismatched product oligonucleotide GGCCCGCU binds to the *Tetrahymena* ribozyme with a K_d of 100 nM at 42 °C (Pyle et al., 1990). Using the gel-filtration assay, the observed K_d was 300 ± 20 nM (Figure 4d), a value 3-fold higher than the K_d determined by other methods. Although this initial application of the method results in a reproducible overestimation of K_d (slightly weaker binding), the method appears to be consistent and accurate for direct determination of RNA–RNA association, particularly under conditions that cannot be studied by other means. The exact value of K_d overestimation by this method and potential remedies for this effect are the subject of ongoing investigations.

Rate Constants from Multiple-Turnover Kinetics. Agreement between K_m(ST) and K_d suggest that D5 and exD123 bind as single, homogeneous populations to form a strong complex. This is because a different RNA (either D5 or exD123) was held limiting in each case and behaved uniformly under those conditions. Agreement between kinetic variables, together with good fit of the single-turnover data to a binding isotherm, also suggests that the maximum rate from single-turnover experiments [k_{cat}(ST)] represents the rate of the chemical step (k_{chem}). Inequivalence between the maximum rate under single-turnover conditions and k_{chem} may still be possible, however, if a rate–limiting conformational change occurs within the D5–exD123 complex. If this were true, then the K_m determined using multiple turnover kinetics [K_m(MT)] might be significantly smaller than K_d and K_m(ST) (Fersht, 1985, pp 102, 109–111). To explore this idea and to determine if similar rate constants could be obtained using a completely different method of analysis, multiple-turnover kinetics of the reaction shown in Figure 1c were conducted by monitoring initial rates of reaction between exD123 in excess using trace, subsaturating concentrations of D5.

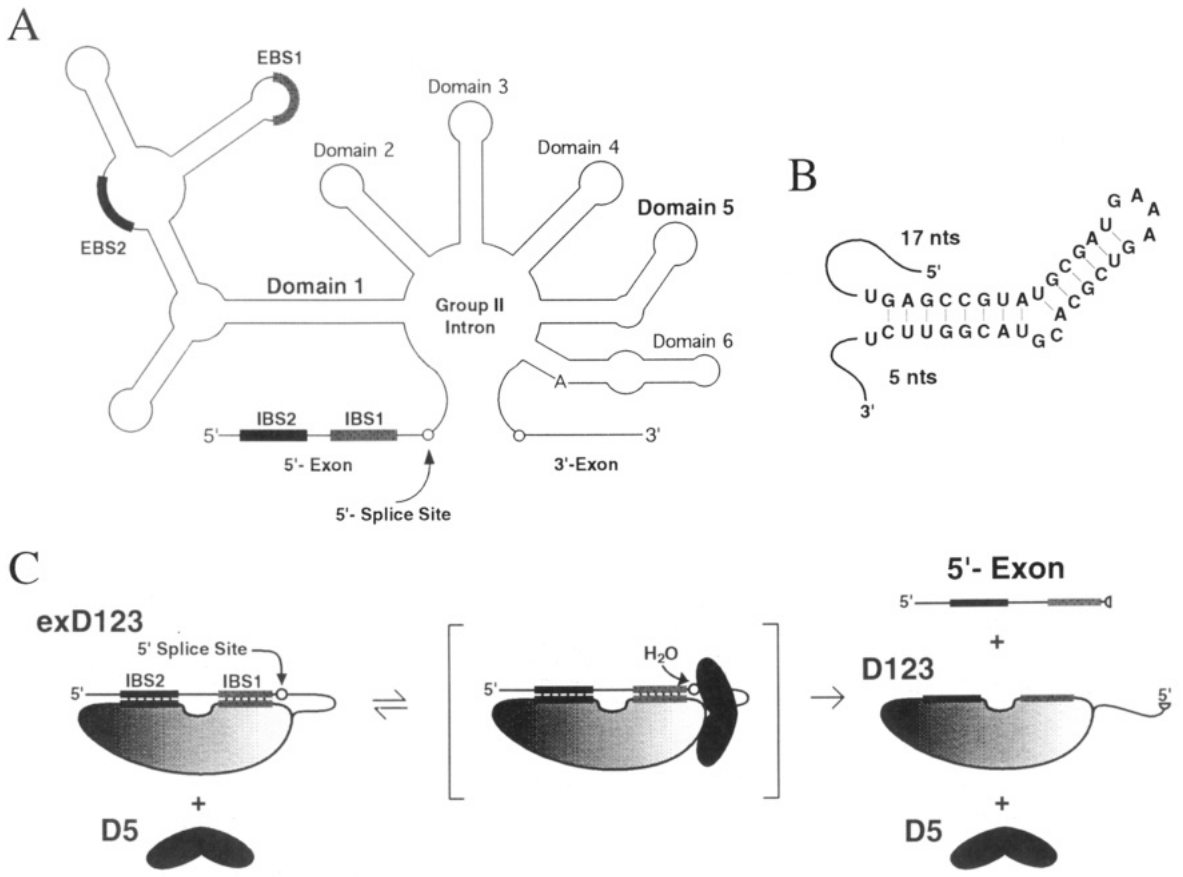

FIGURE 1: Structure and reactivity of the group II intron: (a) Schematic secondary structure of an entire group II intron. The regions of domain 1 (EBS1 and EBS2) that recognize sections of the 5′-exon (IBS1 and IBS2) by base pairing are shown as bold lines (Jacquier & Michel, 1987). Together, domain 1 and domain 5 (shown in bold type) compose the active site for hydrolysis at the 5′ splice site (Koch et al., 1992). The 2′-OH group which attacks the 5′ splice site in full-length introns is located on the bulged adenosine shown in domain 6. This schematic does not illustrate the exact secondary structure of individual domains, which are more complex than indicated here. The exD123 construct used in this study spanned the 5′-exon and much of the intron, ending between domains 3 and 4. Part b shows secondary structure of domain 5 from the ai5γ group II intron. Domain 5 was transcribed as a separate piece of RNA, along with 22 nucleotides of flanking sequences. Part c shows schematic representation of 5′ splice site hydrolysis catalyzed by domain 5 added in trans. The study described here utilized a group II intron in pieces. The exD123 piece, which contains the cleavage site, is composed of the 5′-exon and domains 1–3 of the RNA shown in Figure 1a. The D5 piece is added to the reaction as a separate molecule (shown in b). Water acts as the nucleophile, cleaving the 5′ splice site and generating the products D123 (domains 1–3) and 5′-exon. D5 is released from the reaction unchanged, and is able to catalyze additional rounds of cleavage on other exD123 molecules.

Kinetics were handled as described in Materials and Methods and the results graphed on an Eadie–Hofstee plot (Figure 5). These data fall on a line describing a reaction with K_m(MT) = 190 ± 70.0 nM and k_{cat}(MT) = 0.11 ± 0.028 min^{-1}. The multiple-turnover reaction is difficult to perform and quantitate because long incubations are required to obtain timepoints at high [exD123] and thus there is a higher level of background degradation due to random RNA hydrolysis. This causes rates for the specific cleavage reaction to appear slightly faster, although the 2-fold discrepancy between k_{cat}(ST) and k_{cat}(MT) is relatively insignificant given different methods of determination. Although there is an apparent 4-fold difference between K_m(MT) and K_d values, much of this is probably due to the systematic 3-fold overestimation of K_d using the gel-filtration methodology.

Chemistry Limits the Rate with a Single Proton Transfer. More evidence that k_{cat} represents the rate of the chemical step was provided by a log/linear pH dependence of k_{cat}(ST). By varying pH with rate at saturating [D5], a profile of slope = 1.0 ± 0.17 was observed between pH 5 and 6.2, followed by slow adoption of a plateau that eventually flattens at pH 8.5 (Figure 6). This behavior suggests that the rate is limited by the chemical step of hydrolysis from pH 5 to approximately 7. The profile is similar to that of other reactions in which the chemical rate is limited by proton transfer of a titratable group with pK_a = 7 (Cleland, 1977; Viola & Cleland, 1978). Like many profiles seen with protein enzymes, the log/linear portion of the curve is not followed immediately by flat plateau as in classical examples (Fersht, 1985, p 158). Instead, there is an apparent leveling of the profile from pH 7 to 7.5, after which the profile climbs again. This complex behavior after pH 7.0 may involve an interplay of other titratable groups in the active site or a chemical process other than proton transfer may have become rate-limiting. Alternatively, a partially rate-limiting conformational change that does not involve D5 binding cannot be ruled out. A series of control experiments provides evidence that the observed pH/rate profile is not due to pH-dependent folding or D5 binding effects: When RNAs were "prefolded" in reaction buffer at pH 7.0 and then subjected to a pH jump as D5 and exD123 are combined, the normal pH/rate profile was still observed. Additionally, the same D5 binding profile is observed at both pH 6 and pH 7.5. D5 was found to be saturating at pH 6, 7, 7.5, and 8, ruling out rapid dissociation as a cause for the dip in the profile, although there still may be other conformational effects that we have not eliminated. The log/linear pH/rate profile is consistent with involvement of a titratable group in general base catalysis at the active site. But enzymes commonly have multiple titratable groups and other mechanisms of transition-state stabilization that work in concert, resulting in complicated effects. Additional evidence for a rate-limiting chemical step may be provided through experiments that measure the rate

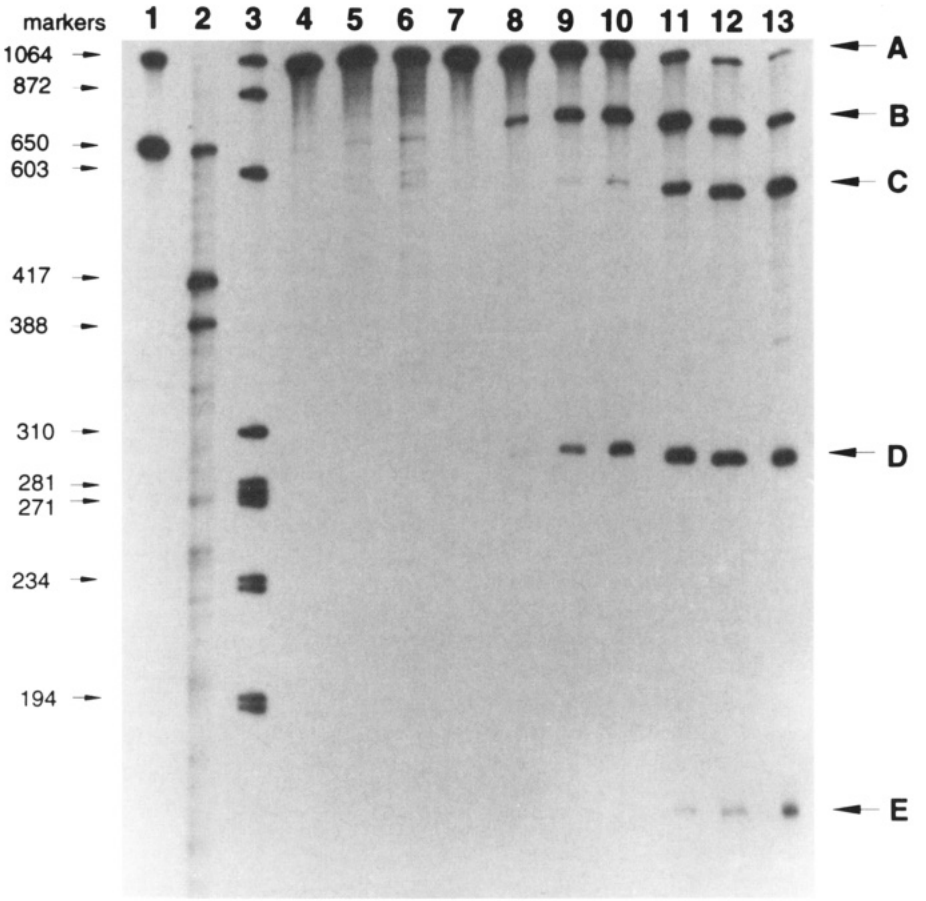

FIGURE 2: The products of 5′ splice site hydrolysis catalyzed by D5. An autoradiograph shows the separation of substrate from product molecules after the reaction shown in Figure 1c. During a reaction containing 1 nM ^{32}P-exD123 and 3 μM D5, aliquots were removed, quenched with denaturant, and run on an 8% denaturing polyacrylamide gel. Band A (1003 nucleotides) is the ^{32}P-exD123 RNA. It is cleaved into 5′-exon (band D, 293 nts) and D123 (band B 710 nts). In a secondary reaction that occurs later, band B hydrolyzes specifically to form bands C and E. Numbers at the far left indicate the size of nucleic acid markers (in nucleotides). Lane 1 contains RNA markers 1064 and 650 nucleotides (nts) in length. Lane 2 contains RNA markers of 650, 417, and 388 nts. Lane 3 contains DNA markers from a ^{32}P-end-labeled *Hae*III digest of ØX174 plasmid DNA which was denatured with urea at 95 °C for 5 min before loading. Lanes 4–6 contain ^{32}P-exD123 RNA (1 nM) incubated for 35, 60, and 120 min, respectively, in the absence of D5 under single-turnover reaction conditions (Materials and Methods). Lanes 7–13 contain ^{32}P-exD123 RNA (1 nM)incubated for 0, 3, 9, 15, 35, 60, and 120 min, respectively, in the presence of 3 μM D5 under standard reaction conditions.

of phosphorothioate cleavage at the active site (Herschlag et al., 1991).

DISCUSSION

Binding between D5 and exD123 RNA is very strong for an interaction stabilized solely by tertiary interactions. The apparent binding constant of D5 to the rest of the group II intron has been examined using several different (and unrelated) methods, all of which are in agreement. Whether measuring the K_m using multiple- or single-turnover kinetics, or directly measuring K_d in a binding assay, D5 binds to the group II intron with an affinity in the nanomolar range (Table 1). This result is consistent with the "high affinity" K_m reported in an earlier study (Franzen, 1993). Because D5 appears to adopt a very stable hairpin structure and there is no phylogenetic covariation between D5 and the rest of the intron, it is likely that this interaction energy stems solely from tertiary interactions such as base triples, base–backbone interactions, or backbone–backbone associations mediated by metal ions. An important role for 2′-OH functionalities in the recognition of D5 by the group II intron active site is supported by the observation that a deoxy-D5 cannot bind exD123 or stimulate chemistry (A. M. Pyle, unpublished results). Collectively, these studies suggest that unusual tertiary interactions can be the sole determinant for association of one folded RNA with another and that RNA–RNA recognition can be mediated by networks of strong, specific tertiary interactions.

The method used for direct determination of binding is novel for RNA studies and merits additional discussion of why it works and why, in its present form, it may result in an underestimation of binding strength. It is important to note that, although we still do not fully understand why gel mobility–shift assays of binding work, they have provided a wealth of information on the thermodynamics of ribozyme–substrate and protein–nucleic acid associations. As in this study, quantitative applications of gel-shift assays were originally based upon empirical agreement with other methods, such as kinetic determinations of K_d. Given that the off-rate of D5 from exD123 is probably faster than the time needed to run the column and the sample is unavoidably diluted during the course of elution, it is suprising that the gel-filtration works unless it preserves a "snapshot" of the equilibrium that existed immediately before loading by rapidly separating bound from free ligand and stabilizing the complex through the course of the elution. With this in mind, one can envision a possible advantage of gel-filtration over gel-shift binding: In the former assay, the complex elutes *first* (in a minute or so), rather than later, as the slower of two species on a native gel that runs for an hour. The stability of the complex during elution is demonstrated by the sharpness of its elution profile, which would tail off if the complex were dissociating. Additionally, the complex does not elute in a greater volume than free ^{32}P-exD123, which elutes as a single species. Apparent complex stability may be due to the fact that the column was run at

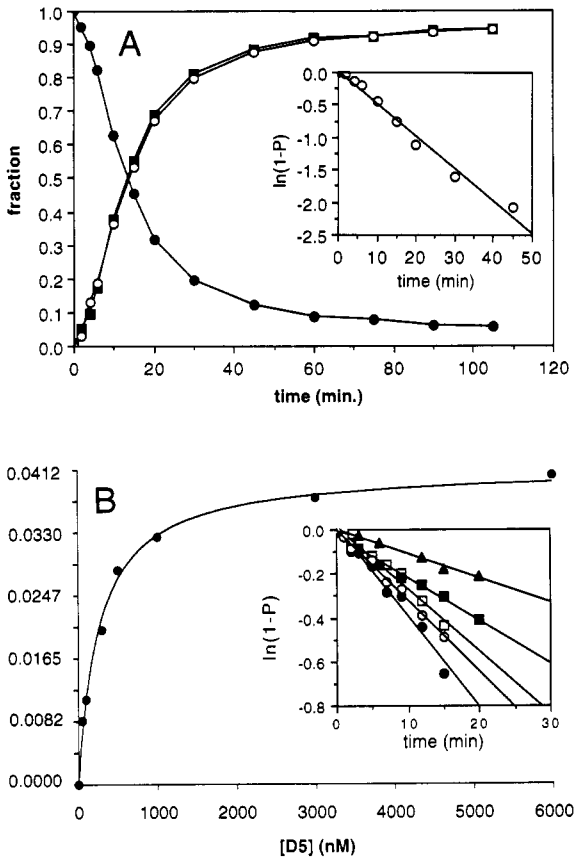

FIGURE 3: Single-turnover kinetics for exD123 cleavage catalyzed by D5: (a) Time course for degradation of exD123 (●) into 5′-exon (○) and D1 RNAs (■) in the presence of excess, saturating D5 (3 μM). The counts in bands B, C, and E (Figure 2) were combined and used to calculate the fraction of D123 product. Plots are superimposable and intersect at 50% reaction. Determination of reaction rate constants (inset): Data is plotted as $\ln(1 - P)$, where P is the fraction of 5′-exon product generated [equivalent to a plot of the ln(fraction of exD123 remaining)]. Plots are linear for more than three reaction half-times ($t_{1/2}$) without end-point correction (shown) and more than five $t_{1/2}$ values if an arbitrary end-point of 95% is chosen. The calculated slope is used to obtain $t_{1/2}$ for the reaction. Values for $k_{obs} = 0.693/t_{1/2}$. For the line shown, k_{obs} was calculated to be 0.050 min^{-1}. Values for k_{obs} varied with a standard error of 18% (at 95% confidence) for identical experiments performed on several days apart. For experiments performed on the same day, variation was considerably lower. Part b shows the determination of K_m(ST) and k_{cat}(ST). By plotting k_{obs} values (inset) as a function of [D5], an apparent Michaelis-Menten binding curve is obtained. K_m(ST) is the [D5] at half-maximum rate and k_{cat}(ST), analogous to k_{chem}, is the maximum rate at D5 saturation, as reported in Table 1. In this experiment, the [^{32}P-exD123] is 1 nM and the [D5] was varied from 50.0 to 6000 nM as shown. Kinetic constants reported here were determined from the fit of the experimental data to a binding equation analogous to that described in the gel-filtration section of Materials and Methods. The equation was adapted by substituting $[exD123]_t$ for $[D5]_t$ and vice versa, K_m for K_d, and k_{obs} for Θ. Substitution of k_{obs} for Θ was made possible by multiplying the right side of the equation by k_{cat}(ST), which is equivalent to the maximum k_{obs} value at the asymptote. In this way, k_{obs}/k_{cat}(ST) is directly analogous to fraction bound. The equation was then solved simultaneously for K_m and k_{cat}(ST) by finding best fit of the equation to the data shown. Several pseudo-first-order plots used to generate the curve are shown (inset). As shown, only data taken at short times (<20 minutes) were used for K_m(ST) analysis. Results for this type of experiment were unaffected by a lack of 95 °C preincubation.

25 °C in order to prevent dissociation. This experimental precaution was based on the fact that many other RNA–RNA interactions studied to date are stabilized by lower temperature. The technique of rapidly lowering temperature after separating bound from free ligand has been successfully applied to the quantitation of large dissociation constants (weak binding) in gel-shift assays (T. Chapman, A. M. Pyle, S.

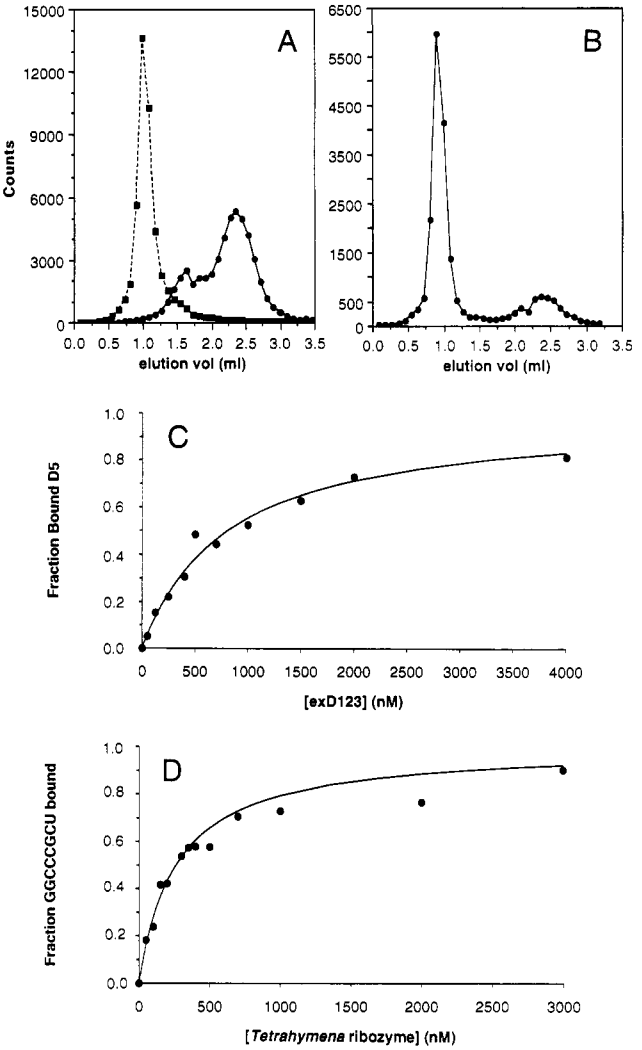

FIGURE 4: Equilibrium binding of exD123 to D5: (a) The large ^{32}P-exD123 (■) molecule elutes faster than ^{32}P-D5 (●) on a gel-filtration column. (b) Incubation of ^{32}P-D5 (●, 16 nM) with unlabeled exD123 (4 μM) results in formation of a complex that elutes rapidly, with the same volume and peak shape as ^{32}P-exD123 shown in a. As expected for equilibrium binding, some unbound ^{32}P-D5 molecules elute in the expected position (~2.3 mL). As shown, the ^{32}P-D5 peak often has a small shoulder. Comparison of a and b shows that this shoulder, like the main peak, decreases on binding exD123 and is therefore unlikely to represent inactive subpopulations *in slow exchange* with the active free population. The subpopulations of D5 which do not elute at 2.3 mL may be active ones, related to conformations involving extra RNA sequences at the 3′- and 5′-ends of the D5 molecule (see Materials and Methods section on DNA constructs and RNA transcripts). When these are removed through use of a new construct encoding just the conserved 36-nucleotide D5, there are no shoulder peaks appearing upon free D5 elution in the presence or absence of exD123 (A. M. Pyle, unpublished results). Part c shows that by titrating ^{32}P-D5 against a range of exD123 concentrations, a binding curve was obtained. There was good agreement between this curve and the standard 1:1 binding equation described in Materials and Methods, resulting in a K_d of 800 ± 50 nM. Part d shows the gel-filtration measurement of GGCCCGCU binding to the *Tetrahymena* ribozyme. GGCCCGCU binds to the *Tetrahymena* ribozyme with a K_d of 300 ± 20 nM using this method. GGCCCGCU was ^{32}P-end labeled and used at a concentration of 1 nM. Concentrations of ribozyme are indicated on the x axis of the plot. These data were fit using the equation and standard error determination described in Materials and Methods, where $[GGCCCGCU]_{total}$ is substituted for $[D5]_{total}$ and $[$*Tetrahymena* ribozyme$]_{total}$ is substituted for $[exD123]_{total}$. Like the K_d of D5 to exD123, the K_d observed for this complex is 3-fold larger than that determined by other methods. Unlike the D5–exD123 binding studies that were conducted using a buffer containing 500 mM KCl and 100 mM $MgCl_2$, the buffer for this titration contained lower salt as required for *Tetrahymena* ribozyme activity: 10 mM $MgCl_2$, 10 mM NaCl, tris pH 7.5; incubation at 42 °C.

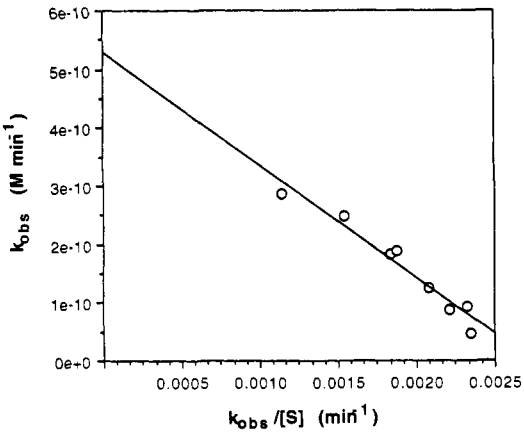

FIGURE 5: Eadie–Hofstee plot of multiple-turnover kinetics results. The apparent rate of reaction (k_{obs}) was plotted as a function of k_{obs}/[substrate] where substrate (S) = exD123. The slope of the line is equal to $-K_m$, the y intercept is equal to V_{max} and $k_{cat} = V_{max}/[E_o]$. The value for E_o, or the total concentration of D5 in these experiments, is 5 nM and the range of exD123 concentrations used in this analysis was 20–250 nM. The best fit of the data was to a line described by the following equation: $y = 5.30 \times 10^{-10} - 1.940 \times 10^{-7}x$, resulting in kinetic constants and standard errors reported in Table 1. Variation between k_{obs} values obtained on different days, with the same RNA stocks, was computed to be ±12% for individual points (with 95% confidence).

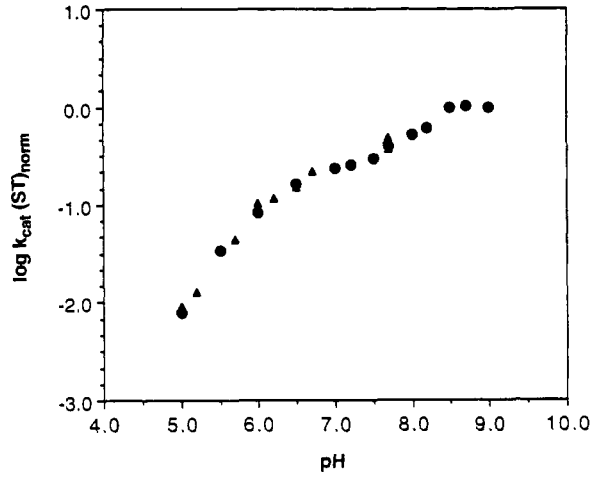

FIGURE 6: The pH/rate profile for k_{cat}(ST). Values for k_{obs} at D5 saturation [k_{cat}(ST), Figure 3b] were obtained from pH 5.0 to 9.0 under reaction condidtions described in Materials and Methods. Rates were normalized to k_{obs} (pH 9.0), the log was taken, and the results [log k_{cat}(ST)$_{norm}$] were plotted vs pH of the reaction. Points designated as ● and ▲ were obtained in separate experiments conducted two weeks apart. The slope of the line between pH units of 5.0 and 6.2 is equal to 1, and an apparent leveling of the profile occurs until it rises again after pH 7.5. This data is consistent with a ribozyme of pK_a approximately equal to 7.0. No reaction was observed below pH 5.0 and prohibitively high levels of RNA degradation were observed above pH 9.0. The error in k_{obs} for experiments performed several days apart under the same experimental conditions was ±18% (with 95% confidence), although k_{obs} varied little between simultaneous experiments.

Moran, T. R. Cech, and D. H. Turner, manuscript in preparation). Additionally, as in gel-shift assays, there may be some loosely defined "cage effect" in the matrix of the sephacryl column which causes released D5 molecules to rapidly bind again before they can be absorbed by the beads and their mobility is altered. While these ideas may help explain why the assay works, they fail to address the problem of 3-fold underestimation binding affinity. The cause of this effect is likely to involve events immediately after loading of the sample. The top 0.5 mm of the column bed is drained of buffer so that the incoming sample drop is immediately absorbed into the matrix with minimal dilution. However, there is probably additional dilution at the moment of loading and the magnitude of this would directly affect K_d in a systematic manner. In spite of these difficulties, this new method warrants serious consideration because it provides information about binding under conditions prohibitive for gel-shift studies. Additionally, it provides a handle on binding that can be used for in vitro selection and discrimination of structural features responsible for complex stabilization.

Scheme 1

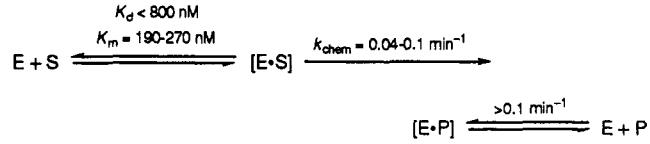

By combining the results of direct binding studies, single-turnover kinetics and multiple-turnover kinetics, a coherent kinetic framework for 5′ splice site hydrolysis emerges. Agreement between K_m and K_d, together with agreement between single- and multiple-turnover analyses, provides evidence that 5′ splice site hydrolysis by D5 is governed by a simple Michaelis-Menten mechanism, and that conformational heterogeneities of D5, exD123, or the D5–exD123 complex do not obscure the chemical rate. K_m(MT) is obtained from rate data that are little affected by [D5] and instead are dependent on the concentration of and conformational homogeneity of exD123. Conversely, K_m(ST) is obtained from rate data little affected by [exD123] and highly dependent on concentration and conformation of D5. Therefore, agreement between K_m(ST) and K_m(MT) suggests that the RNAs are not in slow equilibrium with inactive subpopulations of molecules. The agreement between K_m(ST), K_m(MT), and K_d also implies that the majority of D5 molecules that bind are capable of catalyzing the reaction without rate-limiting conformational changes within the complex (Fersht, 1985, pp 102 and 109–111). For this reason, the values observed for k_{cat} are likely to directly reflect the rate of the chemical step. Due to the levels of uncertainty in our kinetic parameters, we cannot strictly rule out the existence of unfavorable conformations and certainly do not rule out the existence of those that exchange with active molecules at a rate faster than chemistry. Given no evidence for additional steps in the minimal mechanism, our data are consistent with the general mechanistic outline provided by Scheme 1.

The log/linear pH-dependence of k_{cat} provides further evidence that the chemical step is rate limiting, and the pH/rate profile itself has been seen for other enzymes that undergo a form of general base catalysis (Viola & Cleland, 1978). The plot describes a reaction consistent with rate-limiting proton transfer from a titratable group with a pK_a of ≥7.0. We observe a leveling in the profile after pH 7.0 and cannot rule out the possibility that this is due to a rate-limiting conformational change independent of D5 binding. Therefore, a value of 7.0 can be assigned as a lower limit for the pK_a. This apparent pK_a is rather surprising given that ionizable groups in RNA (and on aquated Mg^{2+} ions) fall below pH 3.0 and above pH 10.0. In free solution, there are no groups analogous to histidine with a pK_a of approximately 7.0. However, in the folded core of protein enzymes it is not uncommon for pK_a values to shift dramatically (Cleland, 1977) and this may be a driving force in catalysis by the group II intron active site. We consider a tightly bound Mg-OH to be a general rather than a specific base if it takes part in proton transfer. Despite the apparent role for general base catalysis in this reaction, it is likely that there are other catalytic strategies contributing to transition-state stabilization. There are similarities between

the pH/rate profile shown here and that of a group I intron ribozyme (Herschlag, 1993).

The chemical rate of hydrolysis by this group II intron ribozyme (0.04–0.10 min^{-1} depending on the method of analysis) is comparable to that observed for the *Tetrahymena* ribozyme, derived from a group I intron. The chemical rate for hydrolysis of a 5′ splice site analogue by the *Tetrahymena* ribozyme is 0.7 min^{-1} (Herschlag & Cech, 1990a). Group I and group II introns belong to the same mechanistic class of ribozymes that catalyze nucleophilic attack resulting in products with 3′-OH and 5′-phosphate termini or linkages. In neither case is water the preferred nucleophile for reaction. When the 3′-OH of a bound guanosine cofactor is used in reactions by the *Tetrahymena* ribozyme, k_{chem} proceeds at a respectable 350 min^{-1} (Herschlag & Cech, 1990a). Just as the *Tetrahymena* ribozyme has a "preferred" or natural nucleophile, so does the group II intron, which normally catalyzes 5′ splice site cleavage through attack of the branch-point 2′-OH group located within domain 6. In the group II intron, cleavage at the 5′ splice site may be more rapid when the 2′-OH group of domain 6 is provided as a reaction cofactor. As in the case of guanosine for the group I intron, interactions with domain 6 in the transition state may lower the energy barrier for catalysis and radically stimulate chemical rate.

Just as reaction rate is dependent on pH it is also is directly proportional to the concentration of salt. We studied the raction at 500 mM KCl because it was a practical concentration for setting up reactions. However, values for k_{chem} are directly proportional to [KCl] and would, in fact, be as much as 10-fold faster at the apparent KCl maximum of 2 M (W. L. Michels, unpublished results). Like RNAse P, which can substitute high monovalent cations in vitro for its associated protein in vivo (Reich et al., 1988), the ai5γ group II intron is probably assisted in vivo by a protein cofactor (Lambowitz & Perlman, 1990).

The second-order rate constant for the reaction stimulated by D5 is approximately 100-fold slower than that observed for the *Tetrahymena* and hammerhead ribozymes, which both exhibit values of approximately 10^7 M^{-1} min^{-1} (Fedor & Uhlenbeck, 1990; Herschlag & Cech, 1990a). The value of 10^7 M^{-1} min^{-1} is similar in magnitude to the measured rates of helix formation (Porschke & Eigen, 1971). Because D5 does not recognize exD123 through base pairing to an internal template, it is expected that k_{cat}/K_m would be different than that observed in other ribozymes with an on-rate limited by helix formation. In this case, binding appears to be rapid and chemistry rate limiting, so k_{cat}/K_m values of this ribozyme differ from other systems.

The experiments performed in this study provide no evidence for inactive conformations of either exD123 or D5 that are in slow exchange with active conformations. This observation contrasts with those made in another study reported while this work was in progress (Franzen et al., 1993). Our results might be attributed to the use of standard methods for minimizing inactive RNA populations in studies of ribozyme activity. Anomalies in the behavior of many other ribozymes, even those considerably smaller and less structurally complex than the group II intron, are consistently observed if samples are not preincubated at high temperature and then allowed to fold and cool slowly in the presence of monovalent or divalent cations (Groebe & Uhlenbeck, 1988; Fedor & Uhlenbeck, 1990; Walstrum & Uhlenbeck, 1990). In addition, there are several experimental differences between the standard approach exploited in our study and the kinetics package utilized in the other study. Relative homogeneity in the group II intron substructures studied here indicates that NMR, X-ray diffraction, and other techniques should be readily applicable to the solution of group II intron structural features.

This study demonstrates that it will be possible to identify tertiary interactions stabilizing the active site of the group II intron. It shows that the intron can be kinetically analyzed as a two-piece ribozyme which exhibits multiple-turnover cleavage of a reaction substrate. Like so many other ribozymes, the choice of pieces designated "enzyme" and "substrate" is somewhat arbitrary because domains associate into catalytically active species even if they are not covalently connected. Multiple-turnover catalysis by D5 in trans also has profound implications for the function of group III introns, which may recruit D5 substructures from group II intron segments (Copertino et al., 1992). This approach marks a beginning in the development of a detailed kinetic framework necessary for understanding effects of group II ribozyme structural modifications. Additionally, it may provide a way to examine parallels between the group II intron and other forms of RNA processing.

ACKNOWLEDGMENT

We thank Jennifer A. Doudna for suggesting the use of gel-filtration for measuring interdomain binding, Martha J. Fedor for advice on kinetics, Arthur G. Palmer III for help with statistical analysis, and Dana Abramovitz and Kevin Chin for determining the K_d of GGCCCGCU binding to the *Tetrahymena* ribozyme. We also thank Thomas R. Cech and Daniel Herschlag for critical reading of the manuscript.

REFERENCES

Bachl, J., & Schmelzer, C. (1990) *J. Mol. Biol. 212*, 113–125.
Been M. D., & Cech, T. R. (1987) *Cell 50*, 951–961.
Cantor, C. R., & Schimmel, P. R. (1980) *Biophysical Chemistry; Part II: Techniques for the study of biological structure and function*, W. H. Freeman and Co., San Francisco.
Cech, T. R. (1986) *Cell 44*, 207–210.
Cleland, W. W. (1977) *Adv. Enzymol. 45*, 273–387.
Copertino, D. W., Shigeoka, S., & Hallick, R. B. (1992) *EMBO J. 11*, 5041–5050.
Davanloo, P., Rosenburg, A. H., Dunn, J. J., & Studier, F. S. (1984) *Proc. Natl. Acad. Sci. U.S.A. 81*, 2035–2039.
Fedor, M. J., & Uhlenbeck, O. C. (1990) *Proc. Natl. Acad. Sci. U.S.A. 87*, 1668–1672.
Fedor, M. J., & Uhlenbeck, O. C. (1992) *Biochemistry 31*, 12042–12054.
Fersht, A. (1985) *Enzyme structure and mechanism*, W. H. Freeman, New York.
Franzen, J. S., Zhang, M., & Peebles, C. L. (1993) *Nucl. Acids Res. 21*, 627–634.
Groebe, D. R., & Uhlenbeck, O. C. (1988) *Nucl. Acids Res. 16*, 11725–11735.
Guthrie, C. (1991) *Science 253*, 157–163.
Herschlag, D., & Cech, T. R. (1990a) *Biochemistry 29*, 10159–10171.
Herschlag, D., & Cech, T. R. (1990b) *Biochemistry 29*, 10172–10180.
Herschlag, D., Piccirilli, J. A., & Cech, T. R. (1991) *Biochemistry 30*, 4844–4854.
Herschlag, D., Eckstein, F., & Cech, T. R. (1993) *Biochemistry 32*, 8312–8321.
Jacquier, A., & Michel, F. (1987) *Cell 50*, 17–29.
Jacquier, A., & Jacquesson-Breuleux, N. (1991) *J. Mol. Biol. 219*, 415–428.
Jarrell, K. A., Dietrich, R. C., & Perlman, P. S. (1988a) *Mol. Cell. Biol. 8*, 2361–2366.
Jarrell, K. A., Peebles, C. L., Dietrich, R. C., Romiti, S. L., & Perlman, P. S. (1988b) *J. Biol. Chem. 263*, 3432–3439.
Jencks, W. P. (1987) *Catalysis in Chemistry and Enzymology*, pp 571–574, Dover, New York.

Koch, J. L., Boulanger, S. C., Dib-Hajj, S. D., Hebbar, S. K., & Perlman, P. S. (1992) *Mol. Cell. Biol. 12*, 1950–1958.
Kwakman, J. H. J. M., Konings, D., Pel, H. J., & Grivell, L. A. (1989) *Nucl. Acids Res. 17*, 4205–4216.
Lambowitz, A. M. & Perlman, P. S. (1990) *Trends Biochem. Sci., 15*, 440–444.
Madhani, H. D. & Guthrie, C. (1992) *Cell 71*, 803–817.
McConnell, T. S., Cech, T. R., & Herschlag, D. (1993) *Proc. Natl. Acad. Sci. U.S.A. 90*, 8362–8366.
Michel, F., Umesono, K., & Ozeki, H. (1989) *Gene 82*, 5–30.
Moore, M. J., Query, C. C., & Sharp, P. A. (1993) *The RNA World*, pp 303–357, Cold Spring Harbor Laboratory Press, Cold Spring Harbor.
Mosteller, F., & Tukey, J. W. (1977) *Data analysis and regression; a second course in statistics*, pp 133–139, Addison-Wesley, Reading, MA.
Peebles, C. L., Perlman, P. S., Mecklenburg, K. L., Petrillo, M. L., Tabor, J. H., Jarrell, K. A., & Cheng, H.-L. (1986) *Cell 44*, 213–223.
Porschke, D., & Eigen, M. (1971) *J. Mol. Biol. 62*, 361–381.
Press, W. H., Teukolsky, S. A., Vetterling, W. T., & Flannery, B. P. (1992) *Numerical Recipes in Fortran*, Cambridge University Press, Cambridge.
Pyle, A. M. (1993) *Science 261*, 709–714.
Pyle, A. M., & Cech, T. R. (1991) *Nature 350*, 628–631.
Pyle, A. M., McSwiggen, J. S., & Cech, T. R. (1990) *Proc. Natl. Acad. Sci. U.S.A. 87*, 8187–8191.
Pyle, A. M., Murphy, F. L., & Cech, T. R. (1992) *Nature 358*, 123–128.
Reich, C., Olsen, G. J., Pace, B., & Pace, N. R. (1988) *Science 239*, 117–232.
Sharp, P. A. (1985) *Cell 42*, 397–400.
Sharp, P. A. (1988) *JAMA 260*, 3035–3041.
van der Veen, R., Kwakman, J. H. J. M., & Grivell, L. A. (1987) *EMBO J. 6*, 3827–3831.
Viola, R. E., & Cleland, W. W. (1978) *Biochemistry 17*, 4111–4117.
Walstrum, S. A., & Uhenbeck, O. C. (1990) *Biochemistry 29*, 10573–10576.
Weiner, A. M. (1987) *Cold Spring Harbor Symposia on Quantitative Biology 52*, 933–941.
Wissinger, B., Brennicke, A., & Schuster, W. (1992) *Trends Genet. 8*, 322–328.
Zaug, A. J., Grosshans, C. A., & Cech, T. R. (1988) *Biochemistry 27*, 8924–8931.
Zaug, A. J., McEvoy, M. M., & Cech, T. R. (1993) *Biochemistry 32*, 7946–7953.